Acta Crystallographica Section F
Structural Biology and Crystallization Communications
ISSN 1744-3091

Expression, purification, crystallization and preliminary X-ray diffraction analysis of the DDX3 RNA helicase domain

Bernardo Rodamilans and Guillermo Montoya*

Structural Biology and Biocomputing Programme, Spanish National Cancer Centre (CNIO) Macromolecular Crystallography Group, c/Melchor Fdez Almagro 3, 28029 Madrid, Spain

Correspondence e-mail: gmontoya@cnio.es

Received 12 December 2006
Accepted 6 February 2007

DDX3 is a human RNA helicase that is involved in RNA processing and important human diseases. This enzyme belongs to the DEAD-box protein family, the members of which are characterized by the presence of nine conserved motifs including the Asp-Glu-Ala-Asp motif that defines the family. DDX3 has two distinct domains: an ATP-binding domain in the central region of the protein and a helicase domain in the carboxy-terminal region. The helicase domain of DDX3 was cloned and overexpressed in *Escherichia coli*. Crystallization experiments yielded crystals that were suitable for X-ray diffraction analysis. The final crystallization conditions were a reservoir solution consisting of 2 *M* ammonium sulfate, 0.1 *M* imidazole pH 6.4 plus 5 m*M* spermine tetrahydrochloride and a protein solution containing 10 m*M* HEPES, 500 m*M* ammonium sulfate pH 8.0. The crystals of the helicase domain belong to the monoclinic space group $P2_1$, with unit-cell parameters $a = 43.85$, $b = 60.72$, $c = 88.39$ Å, $\alpha = \gamma = 90$, $\beta = 101.02^\circ$, and contained three molecules per asymmetric unit. These crystals diffracted to a resolution limit of 2.2 Å using synchrotron radiation at the European Synchrotron Radiation Facility (ESRF) and the Swiss Light Source (SLS).

1. Introduction

Higher order RNA structures are formed by intramolecular and intermolecular base pairs that are functionally important. RNA helicases regulate practically all processes in which RNA manipulation is involved, from transcription and translation to nuclear export and RNA degradation (Cruz *et al.*, 1999). They catalyze the modification of higher order RNA structures, such as secondary-structure melting, strand separation and RNA–protein dissociation (Schwer, 2001). Thus, helicases are among the most numerous proteins, with representative members in all three kingdoms of life (Cruz *et al.*, 1999). Even though they are not essential in all cases, they do play a very important role in general RNA metabolism (Rocak & Linder, 2004).

DDX3, also called CAP-Rf (You *et al.*, 1999) or DBX (Lahn & Page, 1997), is a DEAD-box protein of 74 kDa whose precise functions inside the cell are not completely understood. DDX3 bears all nine motifs of the DEAD-box protein family including the characteristic Asp-Glu-Ala-Asp (DEAD box). It has two distinct regions that contain all the conserved motifs. The first region contains the Q-motif (amino acids 178–206; Cordin *et al.*, 2004) and an ATP-binding and hydrolysis domain (amino acids 209–401). This includes motifs I and II (Walker A and B, respectively), Ia, Ib and the motif III that links the ATP binding and hydrolysis to the conformational changes required for helicase activity. The second region consists of the helicase domain (amino acids 412–573) and comprises motifs IV and V. These motifs are probably involved in RNA binding together with motifs Ia and Ib from the first region. Also present in the second region is motif VI, which is believed to participate in ATP binding (Rocak & Linder, 2004). Moreover, the helicase activity of DDX3 has been shown to be dependent on ATP hydrolysis and *vice versa* (Yedavalli *et al.*, 2004).

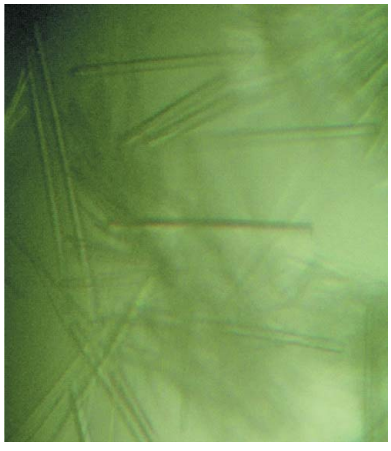

This enzyme is involved in diverse processes such as mRNA splicing by co-localizing with splicing factors (Zhou *et al.*, 2002) and mRNA transport, as it is present in RNA-transporting granules (Kanai *et al.*, 2004). More recently, it has also been described as a tumour suppressor through up-regulation of p21waf1/cip1 (Chao *et al.*, 2006). In addition to its possible implication in proliferation processes, DDX3 is directly involved in other important human diseases that affect large percentages of the world population. This is the case in AIDS, in which DDX3 is upregulated (Krishnan & Zeichner, 2004) and is required for HIV-1 Rev-RRE export from the nucleus (Yedavalli *et al.*, 2004). In hepatitis C, DDX3 is down-regulated (Chang *et al.*, 2006) through a direct interaction with the HCV (hepatitis C virus) core protein during infection, suppressing its RNA-unwinding activity (Owsianka & Patel, 1999; Mamiya & Worman, 1999; You *et al.*, 1999).

Although the structures of other RNA helicases and/or their domains have been solved (Sengoku *et al.*, 2005; Caruthers *et al.*, 2000; Story *et al.*, 2001), there is scant structural information on human RNA helicases and none is available for DDX3. Even though the helicase domain is supposed to be well conserved among the different DEAD-box proteins, an accurate molecular description would be very useful in order to fully understand the molecular mechanisms of RNA unwinding and the interactions of DDX3 with other molecules.

Moreover, the fact that DDX3 is involved in different processes during the development of HIV and HCV viral infections and the possibility that this RNA helicase could function as a tumour suppressor reveal it to be a key regulator of important RNA processes. These crucial roles in RNA metabolism suggest it as a possible drug target in these diseases.

2. Materials and methods

2.1. Protein expression and purification

The cDNA sequence corresponding to residues 407–578 of human DDX3 ($DDX3_{hel}$) was amplified by PCR and cloned into a pCold vector (Takara) using *Nde*I and *Bam*HI restriction sites. A 6×His tag followed by a tobacco etch virus (TEV) protease cleavage site were introduced at the 5′ site. *Escherichia coli* BL21 (DE3) cells were transformed with the pColdIII-$DDX3_{hel}$ vector. Cell cultures were grown at 310 K and induced with 1 m*M* IPTG when the OD reached 0.5–0.8. The temperature was then reduced to 288 K and the cultures were grown overnight. Cells were collected the next morning and the pellets were frozen at 193 K. Upon thawing, a pellet corresponding to 4 l culture was resuspended in 50 m*M* Tris, 500 m*M* ammonium sulfate pH 8.0 (buffer *A*). Cells were disrupted by sonication at 278 K and cell debris was removed by centrifugation. The protein was purified using a 5 ml His-Trap affinity column (Amersham Biosciences). The column was washed with buffer *A* and the protein was eluted with an imidazole step gradient. The eluted $DDX3_{hel}$ was then subjected to proteolytic cleavage with TEV protease at 278 K overnight to remove the 6×His tag. The mixture was again loaded onto a 5 ml His-Trap affinity column (Amersham Biosciences) and the untagged protein eluted in the flowthrough. The sample was collected and loaded onto a gel-filtration column (Superdex 75, Amersham Biosciences) previously equilibrated with 10 m*M* HEPES, 500 m*M* ammonium sulfate pH 8.0. The protein was concentrated to 10 mg ml^{-1} using an ultrafiltration cell (Amicon), flash-frozen in liquid nitrogen and stored at 193 K. The protein purity was analyzed by running a 10% SDS–PAGE gel (Fig. 1*a*) and protein homogeneity was evaluated using dynamic light scattering and mass spectrometry (data not shown). Circular-dichroism spectra and thermal denaturation showed that the protein conserved its secondary and tertiary structure before and after freezing (data not shown). The protein concentration was determined by the Bradford assay (Bradford, 1976; Bio-Rad) using BSA as a standard.

2.2. Crystallization

Crystallization screenings were performed with a Cartesian robot (Genomic Solutions) using the sitting-drop method with nanodrops of 0.1 µl protein solution plus 0.1 µl reservoir solution and a reservoir

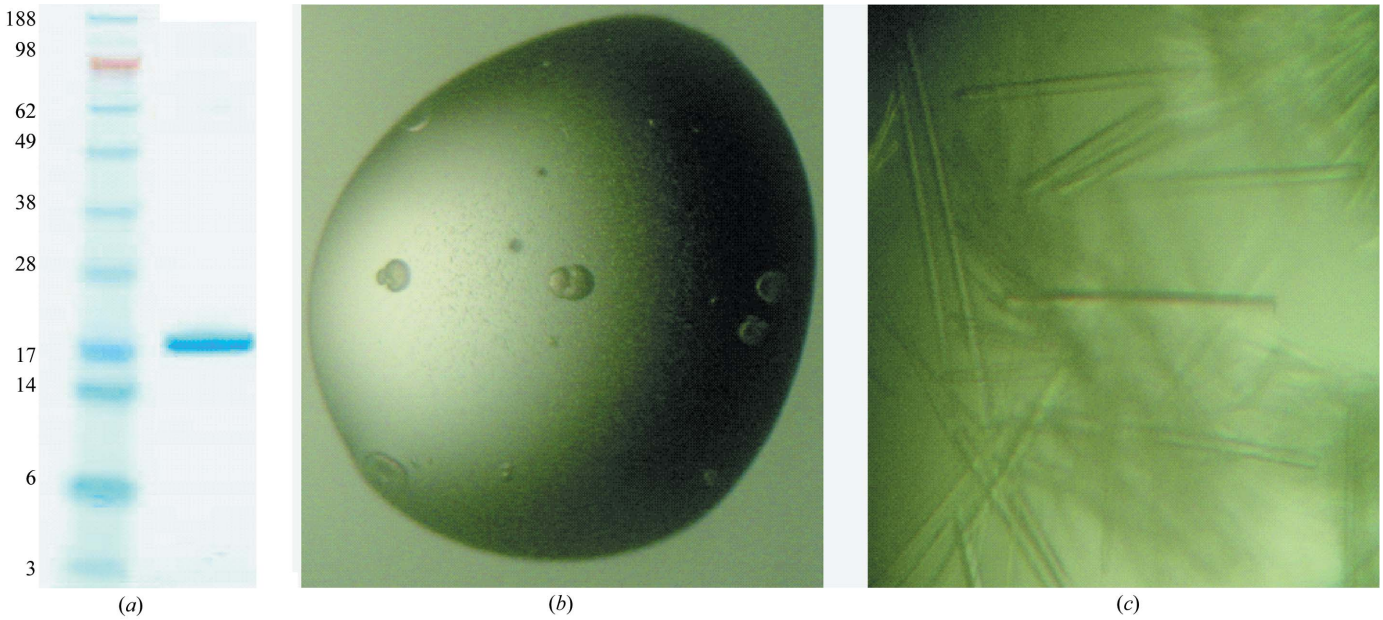

Figure 1
Purification and crystallization of the human DDX3 helicase domain. (*a*) SDS–PAGE of purified and concentrated $DDX3_{hel}$. Left lane, molecular-weight markers (kDa). (*b*) Initial spherulites of $DDX3_{hel}$. (*c*) Monoclinic crystals of $DDX3_{hel}$ obtained from the initial spherulites (see text for details). Crystals of human $DDX3_{hel}$ behaved well in the cryo-buffer conditions described in the text and diffracted to 2.2 Å. The pictures were taken at different magnification settings.

Table 1
Data-collection statistics of human DDX3 helicase domain.

Resolution limits (Å)	$\langle I/\sigma(I)\rangle$	Completeness (%)	Multiplicity	Observed reflections	Unique reflections	R_{sym}†
50.0–6.96	12.9	98.7	6.1	4712	776	0.042
6.95–4.92	11.1	99.2	7.2	9940	1363	0.055
4.91–4.02	10.6	99.4	7.5	13064	1752	0.057
4.01–3.48	8.7	99.4	7.5	15700	2081	0.073
3.47–3.11	6.0	99.4	7.6	17520	2314	0.110
3.10–2.84	3.5	99.3	6.8	17674	2582	0.177
2.83–2.63	2.4	99.3	5.6	15483	2784	0.244
2.62–2.46	1.8	99.2	4.8	14381	2968	0.294
2.45–2.32	1.5	99.1	4.3	13597	3133	0.356
2.31–2.20	1.6	99.0	4.0	13254	3331	0.388
Overall	6.2	99.0	5.9	135325	23084	0.091

† $R_{sym} = \sum_h \sum_i |I_{h,i} - \langle I_h\rangle| / \sum_h \sum_i |I_{h,i}|$.

volume of 70 µl. Initially, small spherulites (Fig. 1*b*) were obtained after 48 h in 0.1 *M* HEPES pH 7.5, 2.5 *M* ammonium sulfate (condition No. 10 from the MbClass II suite screen; Nextal-Qiagen) at 289 K. Refinement of the crystallization conditions was performed at the same temperature using the hanging-drop method in Linbro plates. The reservoir volume was 500 µl and drops were 1 + 1 µl. After several rounds of optimization with different concentrations of precipitant, pH variations and the Additive Screen from Hampton Research, crystals appeared in 2 *M* ammonium sulfate, 0.1 *M* imidazole pH 6.4 plus 5 m*M* spermine tetrahydrochloride in 2 µl drops. Spermine was not critical for crystal formation, but the best data sets were obtained from crystals grown under these conditions. Although many crystals grew in the drop, these specimens could be mounted in a cryoloop. The quality and size (average dimensions 0.2 × 0.01 × 0.01 mm) of the crystals were suitable for diffraction experiments (Fig. 1*c*).

2.3. Data collection and reduction

The $DDX3_{hel}$ crystals were cryoprotected using a buffer consisting of 2 *M* ammonium sulfate, 0.1 *M* imidazole pH 6.4 and 20% glycerol. Crystals were transferred from the original drop to the cryoprotectant drop, incubated for 5 s and then flash-cooled in liquid nitrogen. Although several data sets were obtained in-house using an FR-591 Bruker generator, the crystals only diffracted to 3.8 Å. Therefore, the remainder of the data sets of $DDX3_{hel}$ were collected using synchrotron radiation at the ID14-1 and the PX beamlines at the ESRF (Grenoble) and the SLS (Villigen), respectively. The diffraction data in Table 1 were recorded on an ADSC Q210 detector at ID14-1. The best data set was collected using $\Delta\varphi = 1^\circ$ and a wavelength of 0.9 Å. Processing and scaling were accomplished with *HKL*-2000 (Otwinowski & Minor, 1997); the statistics of the crystallographic data are summarized in Table 1.

3. Results and discussion

The recombinant DDX3 helicase domain (amino acids 407–578; $DDX3_{hel}$) has a molecular weight of 20 kDa. Attempts to purify the full-length protein as well as constructs larger than $DDX3_{hel}$ were initially conducted, but solubility problems led us to try this construct instead. $DDX3_{hel}$ was expressed in *E. coli* with a 6×His tag at the N-terminus, with typical yields of 75 mg pure protein per litre of culture. The recombinant protein was subjected to His-tag affinity purification and the His tag was subsequently removed using TEV protease. The TEV protease was separated from the $DDX3_{hel}$ fragment using another round of His-trap affinity chromatography and a gel-filtration purification step. The purified $DDX3_{hel}$ was concentrated and used for crystallization assays. Although initial hits were just spherulites without crystalline form (Fig. 1*b*), several rounds of refinement allowed us to produce small needles. After optimization, crystals that were suitable in size and quality for diffraction experiments were obtained (Fig. 1*c*). Crystallization reproducibility was very high since only one batch of protein was used for the entire screening and optimization of the crystallization conditions.

The crystals were tested using a synchrotron-radiation source in order to obtain higher resolution data. Several native data sets were collected at 100 K on beamline ID14-1 and the PX beamline at the ESRF (Grenoble) and the SLS (Villigen), respectively. Using synchrotron radiation on these undulator-equipped beamlines, the crystals diffracted to 2.2 Å (Fig. 2). The statistics for a data set are given in Table 1.

The crystals belong to the monoclinic space group $P2_1$, with unit-cell parameters $a = 43.85$, $b = 60.72$, $c = 88.39$ Å, $\alpha = \gamma = 90$, $\beta = 101.02^\circ$. The Matthews coefficient and the self-rotation function (not shown) suggested the presence of three protein molecules per asymmetric unit (V_M = 1.96 Å^3 Da^{-1}) and a solvent content of 37.13%. The collected diffraction data were 99% complete with a multiplicity of 5.9 and an overall $I/\sigma(I)$ of 6.2 (see Table 1 for details). One possibility for solution of the structure of $DDX3_{hel}$ is to use the molecular-replacement method, taking advantage of the previously described structures of Vasa (PDB code 2db3) from *Drosophila melanogaster*, eIF4A (PDB code 1fuk) from *Saccharomyces cerevisiae* and MjDEAD (PDB code 1hv8) from *Methanococcus jannaschii*, all of which are related to DDX3. In case of difficulties, heavy-atom derivatization or selenomethionine-derived protein could be produced to solve the structure using multiple isomorphous replacement (MIR) or multiple anomalous dispersion (MAD) experiments.

These are the first crystals reported of DDX3 RNA helicase. We believe that these studies will help to elucidate the molecular mechanisms of RNA unwinding and the important interactions of this enzyme with different proteins and RNA in the cell. Moreover, owing to the involvement of DDX3 in severe diseases such as AIDS,

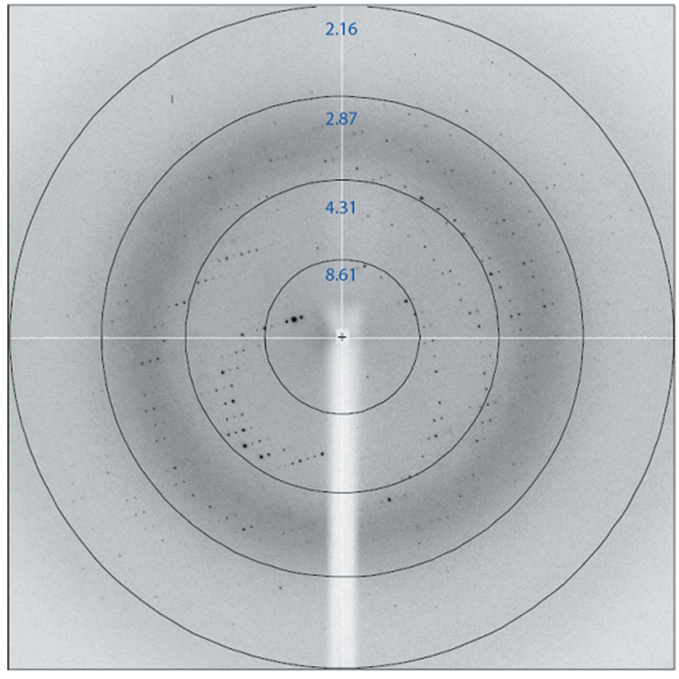

Figure 2
Diffraction pattern from the native crystals using synchrotron radiation at ID14-1 at the ESRF. Circles are labelled with the resolution limits in Å.

hepatitis C and cancer, high-resolution structural information on DDX3 could help in the design of drugs in the search for new therapies.

We would like to thank the personnel of the ESRF and SLS biocrystallography beamlines for their help during data collection. BR thanks the Consejería de Educación de la Comunidad Autónoma de Madrid (CAM) and Fondo Social Europeo (FSE) for a predoctoral fellowship. Financial support was obtained through Ministerio de Educación y Ciencia (BFU-2005-02403, GEN2003-20642-C09-02) grants to GM. We also thank Antonio Rosal for helpful technical assistance.

References

Bradford, M. (1976). *Anal. Biochem.* **72**, 248–254.
Caruthers, J. M, Johnson, E. R. & McKay, D. B. (2000). *Proc. Natl Acad. Sci. USA*, **97**, 13080–13085.
Chang, P. C., Chi, C. W., Chau, G. Y., Li, F. Y., Tsai, Y. H., Wu, J. C. & Wu Lee, Y. H. (2006). *Oncogene*, **25**, 1991–2003.
Chao, C. H., Chen, C. M., Cheng, P. L., Shih, J. W., Tsou, A. P. & Lee, Y. H. (2006). *Cancer Res.* **66**, 6579–6588.
Cordin, O., Tanner, N. K., Doere, M., Linder, P. & Banroques, J. (2004). *EMBO J.* **23**, 2478–2487.
Cruz, J., Kressler, D. & Linder, P. (1999). *Trends Biochem. Sci.* **24**, 192–198.
Kanai, Y., Dohmae, N. & Hirokawa, N. (2004). *Neuron*, **43**, 513–525.
Krishnan, V. & Zeichner, S. L. (2004). *Retrovirology*, **1**, 42.
Lahn, B. & Page, D. (1997). *Science*, **278**, 675–680.
Mamiya, N. & Worman, H. (1999). *J. Biol. Chem.* **274**, 15751–15756.
Otwinowski, Z. & Minor, W. (1997). *Methods Enzymol.* **276**, 307–326.
Owsianka, A. & Patel, A. (1999). *Virology*, **257**, 330–340.
Rocak, S. & Linder, P. (2004). *Nature Rev. Mol. Cell Biol.* **5**, 232–241.
Schwer, B. (2001). *Nature Struct. Biol.* **8**, 113–116.
Sengoku, T., Nureki, O., Nakamura, A., Kobayashi, S. & Yokoyama, S. (2005). *Cell*, **125**, 287–300.
Story, R. M., Li, H. & Abelson, J. N. (2001). *Proc. Natl Acad. Sci. USA*, **98**, 1465–1470.
Yedavalli, V., Neuveut, C., Chi, Y., Kleiman, L. & Jeang, K. (2004). *Cell*, **119**, 381–392.
You, L., Chen, C., Yeh, T., Tsai, T., Mai, R., Lin, C. & Lee, Y. (1999). *J. Virol.* **73**, 2841–2853.
Zhou, Z., Licklider, L., Gygi, S. & Reed, R. (2002). *Nature (London)*, **419**, 182–185.